J Clust Sci (2013) 24:1067–1080
DOI 10.1007/s10876-013-0598-8

ORIGINAL PAPER

Rod-Like Co_2P Nanostructures: Improved Synthesis, Catalytic Property and Application in the Removal of Heavy Metal

Feifei Yuan · Yonghong Ni · Li Zhang · Xiang Ma · Jianming Hong

Received: 11 March 2013 / Published online: 12 June 2013

Abstract In this paper rod-like cobalt phosphide (Co_2P) nanostructures were successfully synthesized at a large scale via an improved water–ethanol mixed-solvothermal route. White phosphorus and cobalt dichloride were used as starting reactants, hexamethylenetetramine as the pH adjustor, sodium dodecyl benzene sulfonate as the surfactant. The reaction was carried out at 170 °C for 800 min. It was found that the morphology and crystallinity of Co_2P nanostructures could be tuned by the amount of hexamethylenetetramine. Experiments showed that the as-prepared Co_2P nanostructures owned good catalytic activity in the reduction of aromatic nitro compounds. Under the presence of 40 mg L^{-1} Co_2P nanostructures, some aromatic nitro compounds, including 4-nitrophenol, 4-nitroaniline, 2,4-dinitrophenol, and 3,5-dinitrosalicylic acid, were fully reduced by $NaBH_4$ within 3–5 min. Also, the catalytic activities of Co_2P nanostructures could be affected by the morphologies of the final products. Furthermore, the as-obtained Co_2P nanostructures also exhibited good adsorption capacities for Pb^{2+} and Cu^{2+} ions in water resources, indicating that the as-prepared product had potential application in environmental treatments.

Keywords Co_2P nanostructures · Catalytic activity · Ion adsorption

F. Yuan · Y. Ni (✉) · L. Zhang
Key Laboratory of Functional Molecular Solids of Education Ministry of China, College of Chemistry and Materials Science, Anhui Normal University, Wuhu 241000, People's Republic of China
e-mail: niyh@mail.ahnu.edu.cn

X. Ma (✉) · J. Hong
Centers of Modern Analyses, Nanjing University, Nanjing 210093, People's Republic of China
e-mail: max@nju.edu.cn

Introduction

Over the past decade, transitional metal phosphides have been attracting increasing research interest in materials science due to their widely potential applications in many fields, including energy source [1, 2], electronic devices [3], information storages [4–6], and photocatalyst [7, 8]. More importantly, it was found that transitional metal phosphides exhibited excellent catalytic activity for hydrodesulfurization (HDS) and hydrodenitrogenation (HDN) [9, 10]. As an important member of transitional metal phosphides, cobalt phosphide has been extensively investigated owing to its interesting magnetic, photocatalytic, and catalytic properties [11].

Generally, transitional metal phosphides consisted of same element bear a variety of phases. For instance, cobalt phosphides include Co_2P, CoP, CoP_2 and CoP_3 [12]. So, it is difficult to prepare nanostructural transitional metal phosphides with definite stoichiometries. Also, the selection of phosphorus source is a key factor in the preparation of nanostructured transitional metal phosphides. Traditionally, highly toxic phosphines (e.g. PH_3) or phosphorus pentachloride were often-used phosphorus sources for the preparation of transitional metal phosphides including cobalt phosphides. Later, trioctylphosphine (TOP) and trioctylphosphine oxide (TOPO) were widely used [13]. In 2005, for instance, Zhang et al. [14] employed TOPO as a controlled phosphorus source for the synthesis of uniform hyperbranched cobalt phosphide nanocrystals. Recently, Yang et al. [15] used Co-TOP as the single-source precursor to successfully obtain Co_xP nanostructures with controlled size, phase, and shape Furthermore, triphenyl phosphine was also used as the phosphorus source for the synthesis of Co_2P nanostructures [16]. However, it was necessary to synthesize transitional metal phosphides at high temperature when the above organic phosphorus compounds were employed as the phosphorus sources. Therefore, it is still urgent to realize the mild preparation of transitional metal phosphide nanocrystals in materials science. Some useful strategies have been attempted. For example, Hou et al. [17] designed a solvothermal route for synthesis of paramagnetic Co_2P nanorods. A mild surfactant-assisted hydrothermal route was also reported for the successful synthesis of rod-like Co_2P nanostructures [18]. Nevertheless, it is still a huge challenge for material scientists to develop a facile and feasible method to prepare morphology- and phase-controlled cobalt phosphide nanocrystals.

In 2009, our group designed a simple water–ethanol mixed-solvothermal route to successfully prepare urchin-like Co_2P nanostructures under the assistance of sodium dodecyl benzene sulfonate at 160 °C for 1000 min, employing white phosphorus (WP) and cobalt dichloride as starting reactants, sodium acetate as the pH adjustor [7]. Experiments showed that the as-prepared urchin-like Co_2P nanostructures could catalytically degrade some organic dyes such as fluorescein and pyronine B under 365 nm UV light irradiation, which exhibited potential applications in environmental treatment and protection. However, the catalytic performance of the as-obtained product for organic reactions was not investigated.

Recently, the reduction of 4-nitrophenol (4-NP) to 4-aminophenol (4-AP) by $NaBH_4$ has become one of the model reactions for evaluating the catalytic activity of various free or immobilized catalysts in aqueous solution [19]. In the current

work, therefore, our interest mainly focused on the catalytic performance of the as-obtained Co_2P nanostructures for the reduction of 4-NP to 4-AP in $NaBH_4$ aqueous solution. To obtain large Co_2P nanostructures with uniform size and shape, we improved the above synthetic route: Hexamethylenetetramine (HMT) was selected as the pH adjustor, and the reaction was carried out at 170 °C for 800 min. Experiments showed that the as-obtained catalyst owned the highly catalytic efficiency for the reduction of some aromatic nitro compounds including 4-NP in $NaBH_4$ solution. Moreover, the as-obtained Co_2P nanostructures also exhibited excellent adsorption capacity for the removal of some heavy-metal such as Pb^{2+} and Cu^{2+} ions from water resources.

Experimental Section

All reagents and chemicals were analytically pure, bought from Shanghai Chemical Company and used without further purification.

Preparation of Co_2P Nanostructures

The preparation of Co_2P nanostructures was similar to our previous report [7]. In a typical experiment procedure, 2 mmol of $CoCl_2{\cdot}6H_2O$ (0.475 g), 0.1 g of sodium dodecyl benzene sulfonate (SDBS, $\sim$0.3 mmol) and 0.2 g of HMT (1.4 mmol) were dissolved in distilled water to form a solution of 8 mL. Then, 12 mL absolute ethanol was added. The mixture was vigorously stirred with a magnetic pulsator at room temperature for 20 min. After the as-prepared solution was poured into a Teflon-lined stainless steel autoclave with capacity of 25 mL, 0.6 g WP was added. Based on the safe consideration, all operations relating to WP were carried out in water. The autoclave was sealed and maintained at 170 °C for 800 min, then allowed to cool down to room temperature naturally. The black precipitates were collected, washed with distilled water and absolute ethanol several times to remove the impurities, and dried in vacuum at 60 °C for 360 min.

The above experimental process was repeated under the same conditions in the presences of HMT with various amounts.

Characterization

X-ray powder diffraction patterns of the products were carried out on a Shimadzu XRD-6000 X-ray diffractometer equipped with Cu Kα radiation ($\lambda = 0.154060$ nm), employing a scanning rate of 0.02° s^{-1} and 2θ ranges from 20° to 80°. The XRD pattern of the product was analyzed by the Rietveld method as implemented in the Fullprof program. TEM image of the product were carried out on a JEOL-2010 high resolution transmission microscope, employing an accelerating voltage of 200 kV. SEM images and EDS analysis of the product were obtained on a Hitachi S-4800 field emission scanning electron microscope, employing the accelerating voltage of 5 and 15 kV, respectively. UV–Vis absorption spectra were recorded on a Hitachi 3010 UV–Vis absorption spectrophotometer.

Catalytic Study

To investigate the catalytic property of the as-obtained Co_2P nanostructures for the reduction of aromatic nitro compounds (4-nitrophenol, 4-nitroaniline, 2,4-dinitrophenol, 3,5-dinitrosalicylic acid), a series of solutions was freshly prepared before experiments. In a typical process, appropriate amounts of aromatic nitro compounds and catalysts were firstly mixed; then, a certain volume of $NaBH_4$ solution was introduced into the system to form a 3 mL of solution. Here, the concentrations of aromatic nitro compounds, $NaBH_4$ and catalyst were 0.5×10^{-4} mol L^{-1}, 2.0×10^{-2} mol L^{-1} and 20–60 mg L^{-1}, respectively. The reductive processes were monitored with a Hitachi 3010 UV–Vis spectrophotometer.

Removal of Heavy-Metal Ions

The as-prepared Co_2P nanostructures could be also used as adsorbents for the removal of heavy-metal ions. 20 mg of Co_2P nanostructures were introduced into a 50 mL mixed solution of Pb^{2+} and Cu^{2+} ions with the initial concentration of 10 mg L^{-1} at room temperature, respectively. The as-obtained mixed system was dispersed by ultrasonic irradiation for 30 min to ensure sufficient interaction between adsorbents and heavy-metal ions. The concentration change of heavy-metal ions before and after adsorption was analyzed by ICP atomic emission spectroscopy.

Results and Discussion

Morphology and Microstructure of Co_2P

Curve 1 given in Fig. 1a is the XRD pattern of the product prepared from the system containing 0.2 g HMT under the present experimental conditions. All peaks can be indexed as the orthorhombic Co_2P phase by comparison with the JCPDS card files no. 32-0306. To further confirm the formation of Co_2P, the XRD data of the product was analyzed by the Rietveld method as implemented in the Fullprof program. Figure 1b shows the Rietveld refinement of the XRD data of the product. The calculated XRD pattern is in good agreement with the experimental one. The rhombohedral crystal structure can be confirmed. The calculated parameters are $a = 5.64895$ Å, $b = 6.60848$ Å and $c = 3.51532$ Å, which are very close to the reported values ($a = 5.646$ Å, $b = 6.609$ Å and $c = 3.513$ Å, no. 32-0306). Furthermore, the energy dispersive spectrometry (EDS) of the as-obtained product also proved the formation of Co_2P (see Fig. 1c). The atomic ratio of Co/P in the nanocrystallines is calculated to be 2.17:1, which is close to the stoichiometry of Co_2P.

The morphology of the final product was observed by SEM and TEM. Figure 2a shows a representative low-magnification SEM image of the product. Rod-like Co_2P nanostructures with uniform size can be clearly seen. Further enlargement shows that the mean diameter and length of nanorods in turn are $\sim$30 and $\sim$200 nm (see the inset in Fig. 2a). Figure 2b depicts a typical TEM image of the product. Some

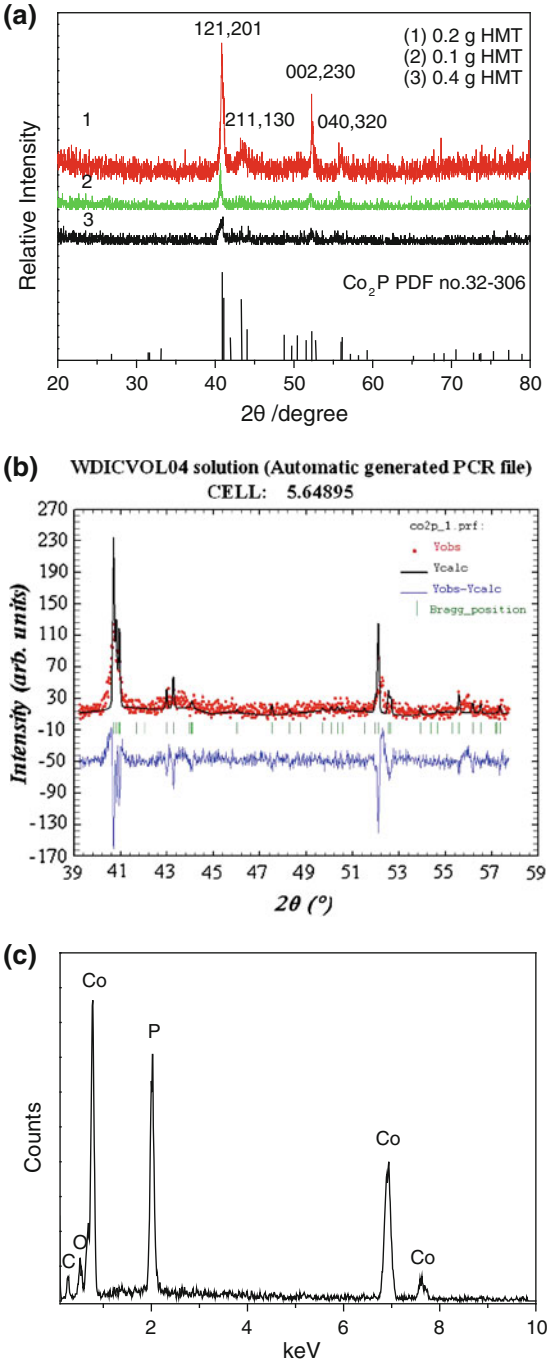

Fig. 1 **a** The XRD patterns of the product prepared from the systems containing various amounts of HMT at 170 °C for 800 min. **b** Comparison between calculated XRD data and experimental data and **c** EDS analysis of the product prepared from the system containing 0.2 g HMT

nanorods with the average diameter of ~30 nm and the length of ~200 nm overlap with each other. This is consistent with the results of SEM observation. A HRTEM image of a nanorod is exhibited in Fig. 2c. The clear stripes indicate the good crystallinity of nanorods. The distance between the neighboring planes is measured to be 0.208 nm, corresponding to the (211) plane of orthorhombic Co_2P. The SAED

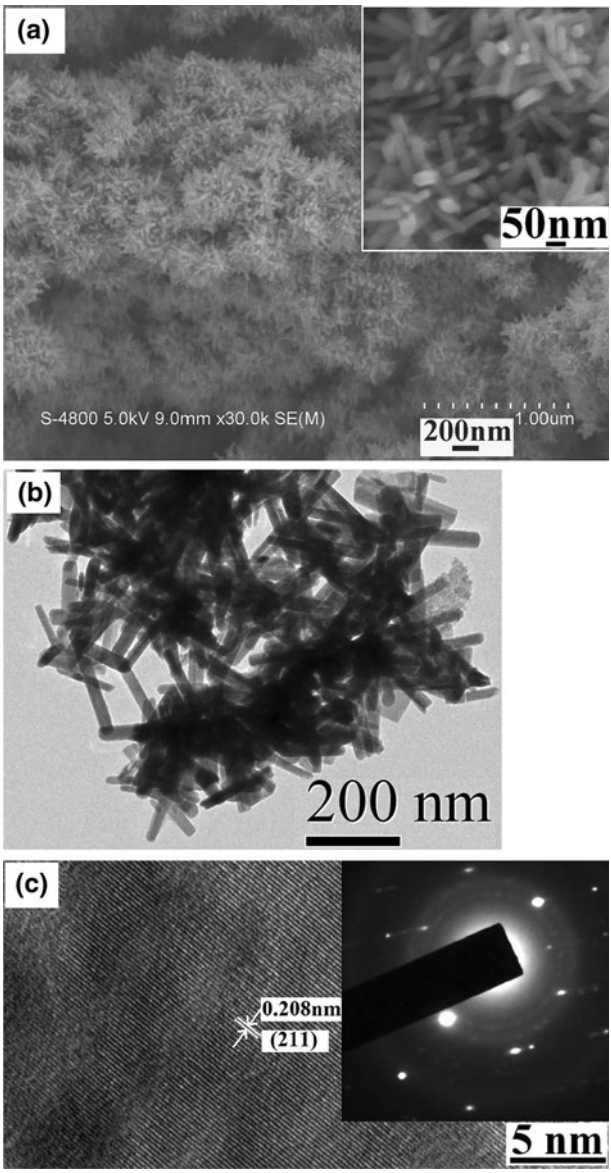

Fig. 2 Electron micrographs of the product prepared by the present mixed solvothermal route at 170 °C for 800 min **a** a low-magnification SEM image (the *inset* is a high-magnification SEM image), **b** a TEM image, and **c** a HRTEM image and SAED pattern

pattern of the nanorods is shown in the inset of Fig. 2c. The clear diffraction dots further confirm the good crystallinity of the product.

Our previous research showed that transitional metal phosphides could be successfully prepared via the dismutation of phosphorus sources from the systems containing water at below 200 °C in the proper pH ranges [7, 18]. Since the dismutation could be promoted in the basic system, metal phosphide nanomaterials were usually prepared in the basic solution. However, the high basicity was unfavorable for controlling the morphology of the product; and also enhanced the reductive ability of phosphorus sources. Therefore, a weak basic environment was usually needed in the synthesis of transitional metal phosphide nanostructures with certain morphologies. In the current work, HMT was selected as the pH adjustor since it could free NH_3 under the lifted temperature. Thus, the pH of the system could be tuned. Experiments showed that only small amounts of aggregated particles were produced when no HMT existed in the system (see Fig. 3a). Meanwhile, most WP remained. After 0.1 g of HMT was introduced into the system, the yield of the product markedly increased. Here, the product was composed of many stubby nanorods and small amounts of tiny nanorods (see Fig. 3b). After 0.2 g of HMT was used, the yield of the product further increased. SEM observations showed that abundant Co_2P nanorods with uniform size were obtained (see Fig. 2a). However, upon further increasing the amount of HMT to 0.4 g, rod-like nanostructures obviously retrograded (see Fig. 3c). XRD analyses confirmed the above SEM results. As seen in Fig. 1a, when the initial amount of HMT was reduced to 0.1 g (curve 2) or increased to 0.4 g (curve 3), the diffraction peaks of the products weakened, implying the bad crystallinities of the products. Distinctly, a proper amount of HMT is necessary in the formation of Co_2P nanorods with uniform size. As mentioned in the previous text, HMT could hydrolyze under the high temperature to produce NH_3, which led to the rise of the pH of the system. Thus, the dismutation of WP was promoted. However, when the amount of HMT was below 0.1 g, the dismutation of WP did not occur or partly occurred owing to the low OH^- ion concentrations, which led to the low yield. While the amount of HMT was above 0.2 g, WP fully reacted to produce more PH_3 within the shorter durations due to the higher basicity. As a result, more Co_2P nuclei were formed, which caused the retrogression of Co_2P nanorods.

Catalytic Property

It was found that the as-obtained product exhibited excellent catalytic activity for the reduction of 4-NP to 4-AP by $NaBH_4$. Usually, the 4-NP aqueous solution presents a strong absorption peak at 317 nm [21]. After $NaBH_4$ is added into the solution, the absorption peak at 317 nm disappears and a new absorption peak at $\sim$400 nm appears. This is attributed to the formation of an intermediate [22]. Based on the electrode potentials of 4-NP/4-AP (−0.76 V) and H_3BO_3/BH_4^- (−1.33 V, vs. NHE) [23], the reductive reaction of 4-NP to 4-AP by $NaBH_4$ should be thermodynamically feasible. In fact, however, the above reaction cannot occur when no catalyst is employed [20]. Namely, it is kinetically restricted in the absence of a catalyst. In practical experiments, the excess $NaBH_4$ is usually used to keep the

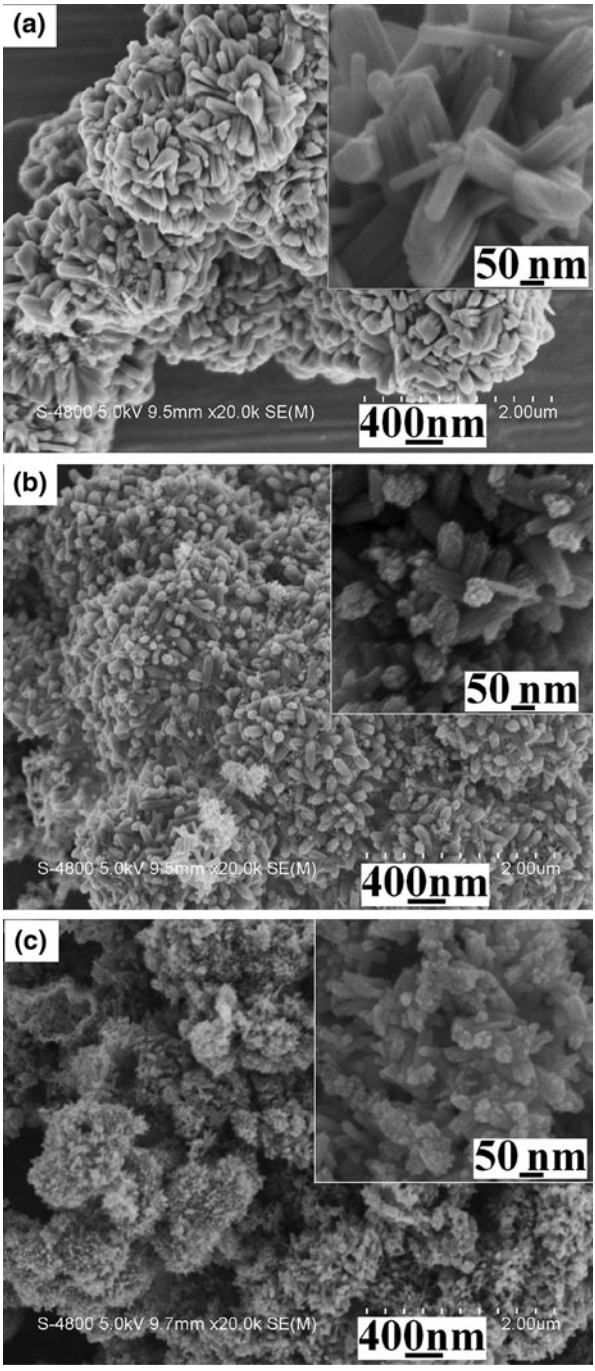

Fig. 3 SEM images of the products prepared from systems with various amounts of HMT at 170 °C for 800 min **a** 0.0 g, **b** 0.1 g and **c** 0.4 g. The *insets* are high-magnification SEM images

concentration of $NaBH_4$ constant during the reduction. Figure 4a exhibits the typical UV–Vis absorption spectra taken at different reaction durations in the presence of 20 mg L^{-1} Co_2P nanostructures. One can clearly see that the intensity of the absorption peak at 400 nm decreases with the prolonging of the reductive time after introducing Co_2P nanostructures into the system. Meanwhile, a new absorption peak at ~307 nm appears, which is the characteristic absorption peak of 4-AP [24]. When the absorption peak at 400 nm disappears, the reductive reaction of 4-NP in $NaBH_4$ solution ends. During experiments, furthermore, we found that the peak intensity of 4-AP at ~307 nm increased at a non-proportional mode. This phenomenon was also observed by Harish et al. [24], and was attributed to the different molar extinction coefficients of 4-NP and 4-AP [24].

Moreover, experiments showed that the reductive rate of 4-NP to 4-AP could be obviously accelerated when the amount of Co_2P catalysts increased. As seen from Fig. 4b, when the amount of Co_2P catalysts increased from 20, 40, to 60 mg L^{-1}, the reductive reaction was completed within 6, 3 and 2 min in turn. The reaction rate was far faster than some reports, in which metal-based catalysts were used [20, 25, 26]. Also, the present reductive reaction was carried out in air and had no inductive time [20]. The above facts indicate that the as-prepared Co_2P nanostructures own outstanding catalytic activity for the reduction of 4-NP to 4-AP in the ambient atmosphere condition.

Further research discovered that the reductive rate of 4-NP to 4-AP could be obviously affected by the morphology of Co_2P. Figure 4c depicts the correlation between the reduction rate and the morphology of the catalyst. As shown in Fig. 3b, c Co_2P nanostructures consisted of stubby nanorods and retrograded nanorods could be obtained in the presences of 0.1 and 0.4 g HMT, respectively. When the above products with the same amount were employed as the catalyst, the reductive efficiencies markedly decreased against Co_2P nanostructures prepared from the system containing 0.2 g HMT. Usually, the activity of a catalyst is related to the number of its active site. The activity of a catalyst decreases with the reduction of the active sites. Based on the SEM images shown in Figs. 2a and 3b, c one can find that aggregated particles are obtained after decreasing or increasing the HMT's amount. This necessarily causes the decrease of the active sites of the catalysts. As a result, the catalytic activities of the catalysts decrease.

Furthermore, we also investigated the catalytic properties of the as-prepared Co_2P catalyst for the reduction of other aromatic nitro-compounds, such as 4-nitroaniline, 2,4-dinitrophenol, and 3,5-dinitrosalicylic acid. Figure 5 shows the concentration changes of the above three aromatic nitro-compounds with the reaction time in the presences of 40 mg L^{-1} Co_2P catalysts, respectively. Distinctly, the present catalyst could also rapidly catalyze the reduction of the above three aromatic nitro-compounds. Nevertheless, the reductive rates of three compounds were different. Under the presence of the catalyst with the same amount, for example, the reductive reactions of three aromatic nitro-compounds were finished within 3 min (2,4-dinitrophenol), 4 min (4-nitroaniline) and 5 min (3,5-dinitrosalicylic acid), respectively. Since the reduction reactions of three aromatic nitro-compounds were carried out under the same experimental conditions, the above differences of reaction rates were possibly related to the structures of three organic compounds.

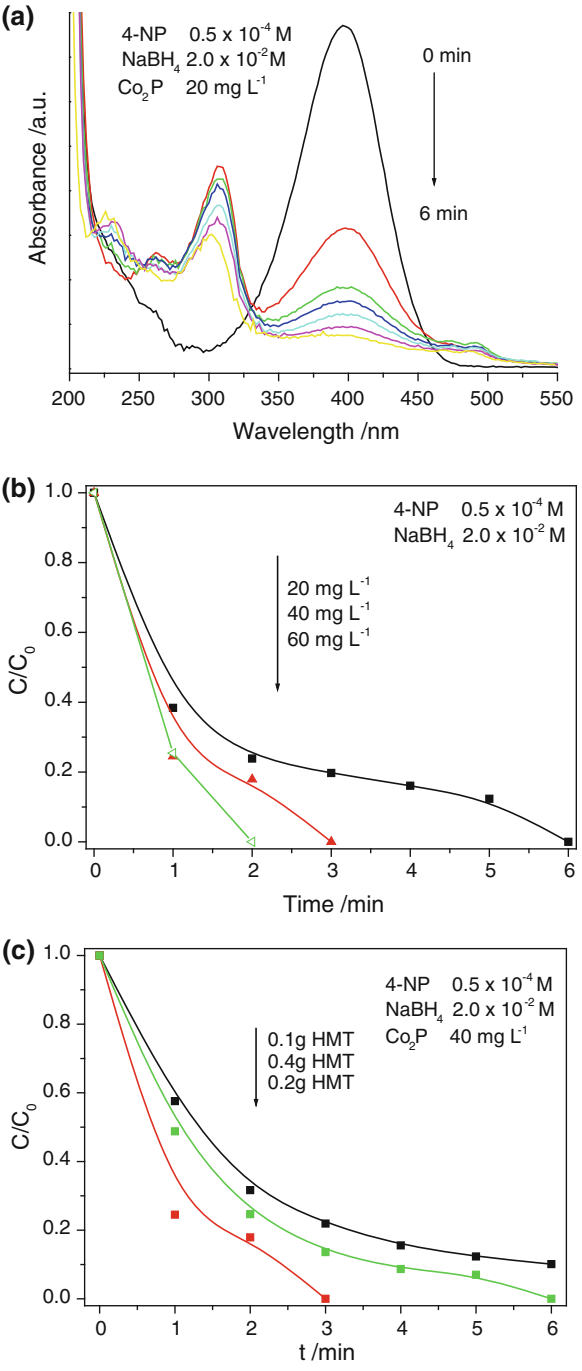

Fig. 4 **a** UV–Vis absorption spectra of the system taken at different reaction durations in the presence of 20 mg L^{-1} Co_2P nanostructures; **b** the influence of the catalyst's amount and **c** the influence of the catalyst's morphology on the rate of the reaction

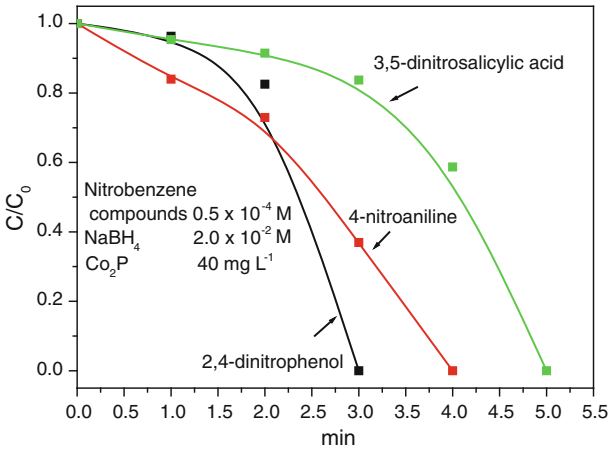

Fig. 5 The concentration changes of various nitrobenzene compounds with the reaction time in the presences of 40 mg L^{-1} Co_2P catalysts, respectively

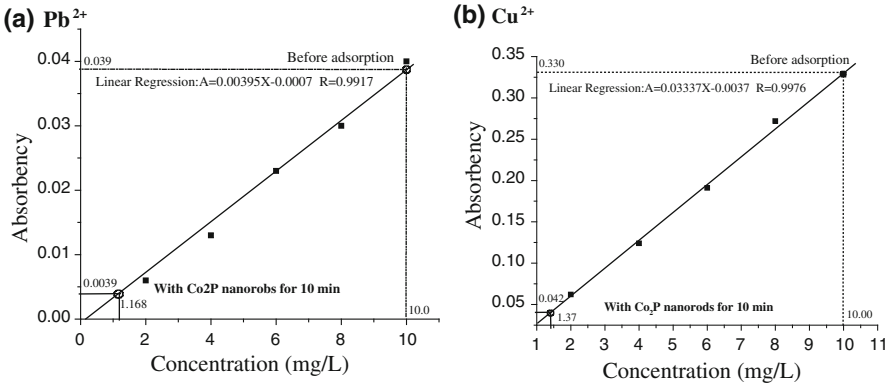

Fig. 6 The absorbency of the solution containing Pb^{2+} **a** or Cu^{2+} **b** ions, respectively: (*dashed dotted line*) calibration curve and (*dotted lines*) before and after adsorption with Co_2P nanorods for 10 min

Removal of Metal Ions

As seen in Fig. 2, the final product was built up of abundant nanorods. N_2 adsorption/desorption experiments showed its BET surface area was $\sim$13.7 m^2 g^{-1}, indicating that the present product probably owned good adsorptive ability. In our previous reports, we found that transitional metal phosphides with certain shapes could be used as adsorbents for the removal of some heavy metal ions, such as Pb^{2+} and Cd^{2+} ions [18, 19, 27]. In the current work, we also investigated the capacity of the as-obtained rod-like Co_2P nanostructures as adsorbents for the removal of these heavy-metal ions from solutions. As shown Fig. 6a, when 20 mg of Co_2P nanostructures were added into a 50 mL mixed solution containing Pb^{2+}, Cu^{2+} ions with the initial concentration

of 10.0 mg L^{-1} at room temperature, the concentration of Pb^{2+} ions changed from 10.0 to 1.168 mg L^{-1} within 10 min. Namely, ~88.3 % of Pb^{2+} ions were removed within 10 min. Here, the adsorption capacity of the adsorbent for Pb^{2+} ions was calculated to be ~22.1 mg g^{-1}, which is far higher than Co_2P nanostructures (17 mg g^{-1}) [18] and porous $Ni_{12}P_5$ superstructures (4.22 mg g^{-1}) [24]. Also, 86.3 % of Cu^{2+} ions were removed under the same experimental conditions and the adsorbent capacity was calculated to be ~21.6 mg g^{-1} (see Fig. 6b). This value is higher than 14.3 mg g^{-1} of porous Ni@C nanocomposites [28]. The above facts indicate that the as-obtained Co_2P nanostructures own excellent ability for simultaneous removals of Pb^{2+} and Cu^{2+} ions from water resources. This should be attributed to the smaller sizes of the as-prepared Co_2P nanorods. Generally, the active sites increase with the size decrease of nanoparticles. Thus, more metal ions

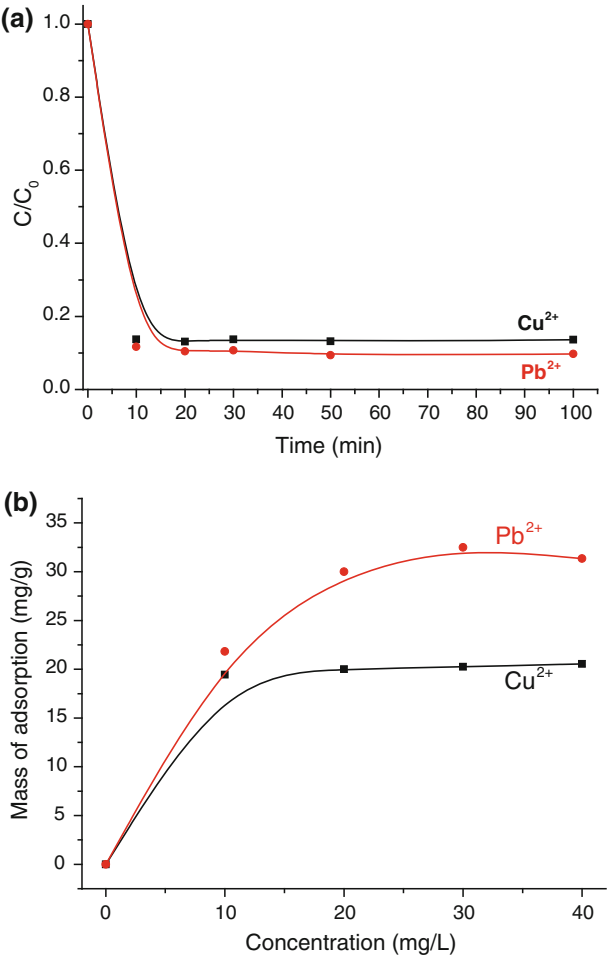

Fig. 7 **a** The concentration changes of various ions with adsorption durations, and **b** the adsorption isotherms of Pb^{2+}, Cu^{2+} ions in the presence of 20 mg Co_2P nanorods

can be adsorbed when the size of the adsorbent decreases. Figure 7a depicts the concentration change curves of the above two ions with the contact time. After adsorption for 10 min, the concentrations of two ions change no longer, implying that adsorbents have reached saturation. The adsorption isotherms of two ions are shown in Fig. 7b. With the increase of initial heavy metal ion concentrations, the removal capacity of Co_2P nanostructures increases till the maximum capacity is reached. Since the concentration of heavy metal ions is usually very low in practical applications, the ability to remove heavy metal ions at low concentrations is a better criterion for selecting a suitable adsorbent. The above experimental results exhibit that the as-produced rod-like Co_2P nanostructures possess outstanding capacities for the fast removals of Pb^{2+} and Cu^{2+} ions, which should have potential applications in the treatment of wastewater.

Conclusions

In summary, rod-like Co_2P nanostructures have been successfully prepared via an improved water–ethanol mixed-solvothermal route in the presence of SDBS. It was found that the yield, crystallinity, and morphology of the final product could be affected by the amount of HMT. Experiments showed that the as-prepared Co_2P nanostructures exhibited the highly catalytic activity in the reduction of aromatic nitro compounds by $NaBH_4$. Under the presence of 40 mg L^{-1} Co_2P nanostructures, aromatic nitro compounds, including 4-nitrophenol, 4-nitroaniline, 2,4-dinitrophenol, and 3,5-dinitrosalicylic acid, could be fully reduced within 3–5 min. Compared with noble-metal-based and Ni–Co alloy catalysts [20, 25, 26], the present Co_2P catalyst owned the higher catalytic efficiency, which presents a potential application in industry as a new-type catalyst for the reduction of aromatic nitro compounds. Furthermore, the as-produced Co_2P nanostructures also showed good adsorption capacities for the fast removal of Pb^{2+} and Cu^{2+} ions from water resources simultaneously. Within 10 min, the removal capacities of the Co_2P nanostructures for Pb^{2+} and Cu^{2+} ions were 22.1 and 21.6 mg g^{-1}, respectively. The above facts indicate that the present product can be used as a promising adsorbent in environmental treatments.

Acknowledgments We thank National Natural Science Foundation of China (21171005) and Key Foundation of Chinese Ministry of Education (210098) for the fund support.

References

1. Y. Lu, J. P. Tu, C. D. Gu, X. L. Wang, and S. X. Mao (2011). *J. Mater. Chem.* **21**, 17988.
2. K. Aso, A. Hayashi, and M. Tatsumisago (2011). *Inorg. Chem.* **50**, 10820.
3. Y. Cui and C. M. Lieber (2001). *Science* **291**, 851.
4. S. L. Brock and K. Senevirathne (2008). *J. Solid State Chem.* **181**, 1552.
5. S. L. Brock, S. C. Perera, and K. L. Stamm (2004). *Chem. Eur. J.* **10**, 3364.
6. Y. Li, M. A. Malik, and P. O'Brien (2005). *J. Am. Chem. Soc.* **127**, 16020.
7. Y. H. Ni, J. Li, L. Zhang, S. Yang, and X. W. Wei (2009). *Mater. Res. Bull.* **44**, 1166.

8. Y. H. Ni, A. L. Tao, G. Z. Hu, X. F. Cao, X. W. Wei, and Z. S. Yang (2006). *Nanotechnology* **17**, 5013.
9. T. Kawai, K. K. Bando, Y. K. Lee, S. T. Oyama, W. J. Chun, and K. Asakura (2006). *J. Catal.* **24**, 20.
10. F. X. Sun, W. C. Wu, Z. L. Wu, J. Guo, Z. B. Wei, Y. X. Yang, Z. X. Jiang, F. P. Tian, and C. Li (2004). *J. Catal.* **228**, 298.
11. I. Lucas, L. Perez, C. Aroca, P. Sanchez, E. Lopez, and M. C. Sanchez (2005). *J. Magn. Magn. Mater.* **290**, 1513.
12. C. M. Lukehart, S. B. Milne, and S. R. Stock (1998). *Chem. Mater.* **10**, 903.
13. J. Park, B. Koo, K. Y. Yoon, Y. Hwang, M. Kang, J. G. Park, and T. Hyeon (2005). *J. Am. Chem. Soc.* **127**, 8433.
14. H. T. Zhang, D. H. Ha, and R. H. Hovden (2011). L. F Kourkoutis, R. D. Robinson. *Nano Lett.* **11**, 188.
15. D. Yang, J. Zhu, X. Rui, H. Tan, R. Cai, H. E. Hoster, D. Y. W. Yu, H. H. Hng, and Q. Y. Yan (2013). *ACS Appl. Mater. Interface* **5**, 1093.
16. N. Zhang, A. X. Shan, R. M. Wang, and C. P. Chen (2012). *CrystEngComm* **14**, 1197.
17. H. W. Hou, Q. Yang, C. R. Tan, G. B. Ji, B. X. Gu, and Y. Xie (2004). *Chem. Lett.* **33**, 1272.
18. Y. N. Ni, J. Li, L. N. Jin, J. Xia, J. M. Hong, and K. M. Liao (2009). *New J. Chem.* **33**, 2055.
19. T. Y. Yu, J. Zeng, B. K. Lim, and Y. N. Xia (2010). *Adv. Mater.* **22**, 5188.
20. S. Saha, A. Pal, S. Kundu, S. Basu, and T. Pal (2010). *Langmuir* **26**, 2885.
21. J. Zeng, Q. Zhang, J. Y. Chen, and Y. N. Xia (2010). *Nano Lett.* **10**, 30.
22. K. Hayakawa, T. Yoshimura, and K. Esumi (2003). *Langmuir* **19**, 5517.
23. S. Jana, S. K. Ghosh, S. Nath, S. Pande, S. Praharaj, S. Panigrahi, S. Basu, T. Endo, and T. Pal (2006). *Appl. Catal. A* **313**, 41.
24. S. Harish, J. Mathiyarasu, K. L. N. Phani, and V. Yegnaraman (2009). *Catal. Lett.* **128**, 197.
25. N. Pradhan, A. Pal, and T. Pal (2002). *Colloid Surf. A.* **196**, 247.
26. K. L. Wu, X. W. Wei, X. M. Zhou, D. H. Wu, X. W. Liu, Y. Ye, and Q. Wang (2011). *J. Phys. Chem. C* **115**, 16268.
27. Y. H. Ni, K. M. Liao, and J. Li (2010). *CrystEngComm* **12**, 1568.
28. Y. H. Ni, L. N. Jin, L. Zhang, and J. M. Hong (2010). *J. Mater. Chem.* **20**, 6430.